Comprehensive Analysis of Differentially Expressed miRNAs in Patients with Ischemic Stroke and Development of a New Risk Prediction Nomogram

Mengxi Gao
The Fourth Hospital of Hebei Medical Univercity
Yan Wang
The Fourth Hospital of Hebei Medical Univercity
Chengyuan Liu
The Fourth Hospital of Hebei Medical Univercity
Lingzhen Meng
The Fourth Hospital of Hebei Medical Univercity
Xiaokun Zhang
The Fourth Hospital of Hebei Medical Univercity
Li Chen
The Fourth Hospital of Hebei Medical Univercity
Qin Zhang
The Fourth Hospital of Hebei Medical Univercity
Liru Guo (qkglrdoctor@126.com)
The Fourth Hospital of Hebei Medical Univercity

Article

Keywords: miRNA, ischemic stroke, qRT-PCR, prediction nomogram, ceRNA

Posted Date: March 18th, 2022

DOI: https://doi.org/10.21203/rs.3.rs-1450575/v1

Abstract

The aim of our study was to investigate the microRNAs (miRNA) associated with ischemic stroke (IS) and developed a new risk prediction nomogram. Gene expression profiles were obtained from public databases. Differentially expressed miRNAs (DEmiRNAs) and differentially expressed mRNAs (DEmRNAs) were identified; Then, the transcription factors (TFs) of DEmiRNAs were predicted and Gene Ontology (GO) analysis and Kyoto Encyclopedia of Genes and Genomes (KEGG) pathway enrichment analysis on DEmRNAs were performed; Then, the miRNA-mRNA network and the competitive endogenous RNA (ceRNA) network were constructed, and the support vector machine (SVM) model was used to further screen key miRNAs. The differential expression of the key miRNAs was verified via experiment. Finally, we combined the patients' disease characteristics and the expression of key miRNAs to construct a risk prediction nomogram. A total of 111 DEmiRNA and 501 DEmRNA were obtained. Top 3 TFs of DEmiRNA were SP1, EGR1 and SP4. GO enrichment analysis on the DEmRNAs showed that they were mainly related to neutrophils and immune activation. Hematopoietic cell lines and cell adhesion molecules were significantly enriched KEGG pathways. MiR-140-3p, miR-34c-5p, miR-330-3p had higher degree in the networks we constructed. In the nomogram, the level of cholesterol, the level of low-density lipoprotein, hypertension, diabetes, the expression of miR-140-3p, miR-34c-5p, and miR-330-3p were related to IS. The current results indicated that hematopoietic cell lineage, cell adhesion molecules, phagosomes, and T cell receptor signaling pathways were important pathways in IS. MiR-140-3p, miR-34c-5p, and miR-330-3p may play a pivotal role in the pathogenesis and progression of IS, and may be potential new therapeutic targets for IS.

Introduction

Stroke is an acute cerebrovascular disease, which displays various clinical features caused by blood vessels in the brain occlusion or bleeding[1]. Stroke is mainly divided into ischemic stroke (IS) and hemorrhagic stroke, IS accounts for the majority. This cerebrovascular disease is the leading cause of disability worldwide and among the leading causes of death[2]. Currently, the diagnosis of IS is mainly based on clinical examination. Such as magnetic resonance imaging (MRI) and computed tomography (CT)[3]. However, the disadvantages of being expensive and not easily available limit CT and MRI as tools for stroke diagnosis. At the same time, IS still lacks an ideal treatment method, and early detection of high-risk groups is the key to IS prevention. Therefore, there is an urgent need for blood biomarkers for IS and IS risk assessment.

MicroRNA (miRNA) is an endogenous single-stranded non-coding micro RNA molecule. It plays an important role in regulating gene expression[4] and a series of physiological and pathological functions such as development, differentiation, apoptosis, and metabolism. In addition, miRNA are abundant in the nervous system, which may be related to neurodevelopment and function[5]. In recent years, the use of miRNAs as new markers for clinical diagnosis of diseases has aroused great interest [6,7]. And some

studies have explored circulating miRNAs can be used as useful biomarkers for IS, such as miRNA-30a, miRNA-126, let-7b[8], miRNA-124-3p and miRNA-16.

lncRNA is a non-coding RNA with a length greater than 200 nucleotides. It can be used as a competitive endogenous RNA (ceRNA) to adsorb miRNA and participate in the regulation of target expression. CeRNA refers to RNA that has sites that can compete with miRNA to bind miRNA, thereby inhibiting miRNA's regulation of the target.

In this study, we performed a comprehensive analysis of miRNA and mRNA expression by reanalyzing the GSE55937 and GSE16561 public data sets. Compared with the control group, differentially expressed miRNAs (DEmiRNAs) and mRNAs (DEmRNAs) were screened. The transcription factors (TFs) of DEmiRNAs were enriched, and DEmRNAs were functionally annotated. Next, we predicted the interaction between DEmiRNA and DEmRNA, and demonstrated them by constructing a regulatory network and a ceRNA network. At the same time, we recruited patients and proved the expression of important miRNAs in the network through quantitative reverse transcription polymerase chain reaction (qRT-PCR) experiments. We hope to find new IS biomarkers. In addition, we have built a simple but effective IS risk prediction tool on these basis, using only the features that are easily available at the beginning of the consultation to assess the risk of disease.

Materials And Methods

Data source.

The GSE55937 and GSE16561 datasets used in our study were downloaded from the Gene Expression Omnibus (GEO) database[9] (https://www.ncbi.nlm.nih.gov/geo), and the search keyword was "Ischemic stroke". The miRNA data set GSE55937 contains 24 ischemic stroke samples and 24 control samples. The gene expression profile GSE16561 contains 39 patients diagnosed with IS by MRI and 24 patients with non-stroke neurologically healthy people. GSE55937 were selected to construct the support vector machine (SVM) model.

Screening DEmiRNAs.

GEO2R (https://www.ncbi.nlm.nih.gov/geo) is an easy-to-use online tool that can identify DEmiRNAs. GEO2R will automatically calculate the false discovery rate (FDR) and detect miRNAs with statistical significance ($P<0.05$) by multiple t test and FDR correction.

Targets prediction of DEmiRNAs and enrichment of TFs.

FunRich[10](version 3.1.3, http://www.funrich.org/) is an open access analysis tool. It allowed functional enrichment analysis of gene and protein background databases. In our study, we used FunRich to predict targets and enrich TFs of DEmiRNAs.

Screening and functional annotation of DEmRNAs.

DEmRNAs was extracted with the "Limma" package (version 3.6.3, https://www.r-project.org/) in R software taking the adjusted p-value <0.05 as the selection criterion. The Gene ontology (GO) database was established by the Gene Ontology Federation in the 1990s. GO mainly contains three parts: biological processes (BP), cell composition (CC) and molecular functions (MF)[11]. The Kyoto encyclopedia of genes and genomes (KEGG) was used to understand the advanced functions of biological systems[12,13]. GO and KEGG enrichment analysis, belong to functional annotation, were conducted by "org.Hs.eg.db" package in R software.

Construction of DEmiRNAs-DEmRNAs regulatory network and ceRNA regulatory network.

The predicted targets of DEmiRNAs and DEmRNAs were intersected and screened for negatively related miRNA-mRNA relationship pairs. Cytoscape software (version 3.6.1, https://cytoscape.org/) was used to construct miRNA-mRNA regulatory network. Next, we used the miRNA-lncRNA relationship pairs in the Starbase database[14](http://starbase.sysu.edu.cn/index.php) to screen for lncRNAs that interacts with DEmiRNAs. The screening criterion was medium stringency ≥2. According to the predicted relationship pairs to construct the competitive endogenous network (ceRNA).

SVM Model Prediction

Support vector machine (SVM) was first proposed by Cortes and Vapnik[15]. It is a supervised machine learning algorithm . Its main idea is to establish a hyperplane as a decisionsurface in order to determine whether the key miRNAs in the network can be used as biomarker. GSE55937 including 24 IS patients and 24 healthy controls was selected for the construction of SVM models. The expression of three key miRNAs (miR-34c-5p、miR-140-3p、miR-330-3p) in different samples was used as the feature values for classification prediction. We use MATLAB environment for SVM implementation. The prediction efficiencies of the model were evaluated through receiver operating characteristic (ROC) curve.

Experimental verification

The whole blood samples of all participants came from the XXXX Hospital. All procedures performed in this study were in accordance with the ethical standards of the Helsinki Declaration of 1975 and Amendments. The research procedure was approved by the Ethics Committee of the Fourth Hospital of Hebei Medical University (document number: 2020142).

RT-qPCR was used to verify the DEmiRNAs in IS patients and healthy controls. In short, using RNA Express Total RNA Kit (Cat. No: M050; NCM Biotech, Suzhou, China) from 40 patients with IS (IS group) and 40 healthy volunteers (normal controls group) total RNA was extracted from peripheral blood, and complementary DNA (cDNA) was synthesized using CellTiter 96 AQueous One Solution Cell Proliferation Assay (Promega LOT: 0000482555) kit according to the manufacturer's protocol. RT-qPCR was performed in a quantitative PCR reactor (CFX96 Touch;Bio-Rad Laboratories, Inc.). We selected 4 patients in each group for qPCR. These 4 patients in each groups were matched by age and gender and had similar lesions to choose. The reaction system includes cDNA, Mix, PCR forward primer and PCR reverse primer.

The primers for the three miRNAs are summarized in Supplementary table 1. Use the 2-ΔΔCt square to calculate the expression level of miRNA. U6 was used as an internal control.

Statistical analysis

Statistical analysis was done by SPSS software package (version 25) (SPSS Inc., Chicago, IL, USA) and GraphPad Prism Version 8.0.1 (GraphPad Software Inc., SanDiego, CA) and R software (Version 4.1.2). Normally distributed data are expressed as mean and standard error. Data of the two study groups were analyzed with independent samples test. Categorical variables were compared using chi-square test. A value of $p < 0.05$ was considered to be a significant difference. The least absolute shrinkage and selection operator (LASSO) method is suitable for the reduction in data[16,17]. Features with non-zero coefficients in the LASSO regression model were selected[18]. Then, a multivariate logistic regression analysis was used to build a predictive model. Variables related to disease were included. All potential predictors were used to develop predictive models of IS risk through the use of cohorts[19,20]. In order to quantify the performance of the predictive nomogram, Harrell's C index was measured. The nomogram model was internally validated by sampling 1,000 times and the relative corrected C-index was calculated[21].

Results

Identification of DEmiRNAs and DEmRNAs.

111 DEmiRNAs (76 up-regulated and 35 down-regulated) (Supplementary 1) and 501 DEmRNAs (258 up-regulated and 243 down-regulated) (Supplementary 2) were identified. Then we found the targets of miRNAs by FunRich software.

Enrichment of TFs.

Entered 111 DEmiRNAs in FunRich to obtain TFs. The figure 1 showed the top 10 TFs, the degree of enrichment and the proportion of miRNAs. The top 10 TFs included SP1, EGR1, SP4, POU2F1, RREB1, TCF3, TFAP4, NFIC, SOX1, KLF7 .

Functional annotation of DEmRNAs.

Neutrophil activation, neutrophil mediated immunity, neutrophil degranulation, neutrophil activation involved in immune response were significantly enriched GO terms. The most significantly enriched BP, CC, and MF terms in stroke were neutrophil activation, secretory granule membrane, and pattern recognition receptor activity (Figure 2). The most significantly enriched KEGG pathway in stroke were: hematopoietic cell lineage, cell adhesion molecules, phagosome, T cell receptor signaling, Th17 cell differentiation and B cell receptor signaling (Figure 3).

Construction of miRNA-mRNA and ceRNA regulatory network.

We obtained 14 pairs of DEmiRNA-DEmRNA, including 5 up-regulated and 1 down-regulated miRNAs, and 2 up-regulated and 12 down-regulated mRNAs (Figure 4). By predicting the lncRNA of all 6 miRNAs in the regulatory network, four miRNA-lncRNA relationship pairs were obtained, including 4 miRNAs and 3 LncRNAs. We compared the role of these four miRNAs in the miRNA-mRNA regulatory relationship and integrated with the interaction of miRNA-lncRNA to obtain a total of 15 relationships (Figure 5).

Patient characteristics

40 patients with IS admitted to our hospital from December 2020 to June 2021 were collected as the experimental group, and 40 volunteers were collected as the control group. The characteristics of the IS group and control group were shown in Table 1. We recorded age and gender, risk factors, and important laboratory data for all subjects.

There was a statistically significant difference between the IS group and the control group in terms of cholesterol, low density lipoprotein levels, high blood pressure and high blood sugar.

The SVM Model Prediction Results

To determine whether plasma miRNA can be used as biomarkers for clinical applications. Through SVM model prediction, three miRNAs, miR-34c-5p, miR-140-3p, and miR-330-3p were used as markers, and ROC curve was used to predict the efficiency of the model. The area under the curve (AUC) was 0.8056. (Figure 6).

Experimental verification

The qRT-PCR method was used to verify the expression levels of three miRNAs used in the construction of the SVM model. QRT-PCR results showed that the relative expressions of miR-34c-5p, miR-140-3p, and miR-330-3p in the IS group were significantly higher than those in the control group ($P< 0.01$). As shown in Figure 7.

Feature selection

6 potential predictors characteristics included the level of cholesterol, the level of low-density lipoprotein, hypertension, the expression of miR-34c-5p, miR-140-3p, and miR-330-3p.As shown in Figure 8.

Predictive model establishment

Developed a model for the level of cholesterol, level of low-density lipoprotein, high or low blood pressure, miR-34c-5p, miR-140-3p, and miR-330-3p expression models and expressed them as alignments Figure (Figure 9).

The risk nomogram in the cohort is used to predict the risk of IS It showed good agreement in this cohort (Figure 10). The C index of the predictive nomogram of this cohort is 0.997, and it is confirmed to be

0.980 through guided verification, which indicates that the model has good discrimination ability. In the disease risk nomogram, the apparent performance indicates a good predictive ability.

Discussion

IS often causes a strong neuroinflammatory response and oxidative stress response, which causes irreversible neuronal damage and disability in patients. Although blood vessels can be recanalized clinically, cerebral ischemia reperfusion itself usually causes neuronal damage to be difficult to recover[22]. Reducing inflammation and oxidative reactions provides new ideas for the prevention or treatment of cerebral ischemia-reperfusion injury[23]. However, there is still a lack of effective targets for down-regulating inflammation, oxidative stress and the resulting neurodegeneration. In our study, we mainly focused on the role of key miRNAs in patients with IS.

We first screened the changes in mRNA and miRNA expression profiles of patients with IS through the analysis of public databases. We found 111 DEmiRNA and 501 DEmRNA. The highly enriched TFs of DEmiRNAs include SP1, EGR1, SP4 and so on. The GO enrichment of DEmRNAs is mainly distributed in two categories: activation of neutrophil activity and activation of immune response. Further KEGG enrichment revealed several important pathways, including hematopoietic cell lineage, cell adhesion molecules, phagosomes, and T cell receptor signaling. Animal experiments have shown that stroke activates hematopoietic cells by increasing sympathetic tone[24]. Anti-adhesion agents also seem to expand the therapeutic window of thrombolytic therapy[25]. In systemic infections and traumatic brain injuries, transient disturbances in the phagocytic function of phagocytes and related bactericidal mechanisms have been detected[26,27]. The immune changes caused by stroke can impair the defense function of phagocytes against bacteria. These changes increase the chance of infection[28], and T cells respond to the protective effects of acute inflammatory injury and acute stroke[29]. Animal experiments have shown that B-cell-deficient mice have a larger infarct area and more severe functional defects, suggesting that enhanced B-cell regulation may be a new way to treat this destructive neurological disease[30]. In conclusion, we believe that hematopoietic cell lineage, cell adhesion molecules, phagosomes, and T cell receptor signaling pathways may play an important role in the pathogenesis of IS.

MiR-34c-5p, miR-125a-5p, miR-455-5p and miR-361-5p have high expression levels in the construction of miRNA-mRNA regulatory network and ceRNA regulatory network. Further SVM model construction, screening miR-34c-5p, miR-140-3p, miR-330-3p can be used as disease prediction markers. At the same time, we recruited patients and healthy volunteers, collected peripheral blood, and tested the expression levels of key miRNAs. The results of the experiment were consistent with the previous bioinformatics analysis. In addition, we had developed a nomogram that can be used to predict the probability of illness based on the information that are easy to collect when visiting a doctor and the relative expression of important miRNAs. The internal verification in the queue showed good discrimination ability.

Hsa-miR-140-3p is a microRNA related to the regulation of inflammation, oxidative stress and apoptosis[31,32]. In recent reports, miR-140-3p has played a pathogenic or protective role in a variety of diseases, including myocardial infarction[33], hyperglycemia[34], skeletal dysplasia [35], equine metabolic syndrome [36], neonatal repetitive pain[37], stent restenosis, and coronary artery disease[38]. Importantly, it was found that miR-140-3p is involved in the regulation or imbalance of oxidative stress and apoptosis in myocardial infarction[39,40]. This disease has many similarities with IS.

It has been reported that miR-34c-5p directly regulates the expression of soluble guanylate cyclase β under the induction of hypoxia. They found that the key TF Sp1 controls the expression of miR-34c-5p during hypoxia[41]. The latest research also proved that overexpression of miR-34c-5p can improve cerebral infarction in a rat model of middle cerebral artery occlusion, and miR-34c-5p plays an important role in cerebral ischemia/reperfusion injury [42]. MiR-330-3p has become a therapeutic target and biomarker for neurological diseases[43]. Inhibition of miR-330-3p inhibits the progression of neuropathic pain by inhibiting neuro-inflammation in the body[44]. However, the further mechanism of anti-inflammatory of miR-140-3p, miR-34c-5p, miR-330-3p, anti-oxidative stress or anti-apoptotic effects should be further studied.

miR-140-3p, miR-34c-5p, miR-330-3p have a high degree in the network we constructed. Experiments verified that the expression of miR-140-3p, miR-34c-5p, and miR-330-3p is higher in the IS population. These miRNAs also play an important role in the pathogenesis and progression of IS. They may be potential new therapeutic targets for cerebral ischemic stroke.

Nowadays, nomograms are widely used in medicine field. The nomogram leverages a simple numerical interface, higher accuracy, and easier-to-calculate predictions to help make better clinical decisions[45]. Our research has developed and validated a new predictive tool that uses only four readily available variables and the relative expression levels of key miRNAs to assess the risk of IS in patients. In the analysis of risk factors, the level of cholesterol, the level of low-density lipoprotein, high blood pressure, diabetes, the expression status of miR-34c-5p, miR-140-3p, and miR-330-3p may be related to the disease status of patients with cerebral infarction. The nomogram shows that high cholesterol content, high low-density lipoprotein content, high blood pressure, diabetes, relatively high expression of miR-34c-5p, miR-140-3p, and miR-330-3p may be key individual factors in determining the risk of IS. This is similar to previous research[46,47]. Higher level of low-density lipoprotein is also associated with higher risk of disease. The study showed that patients with relatively high expression of key miRNAs, miR-34c-5p, miR-140-3p, and miR-330-3p are more likely to suffer from cerebral infarction.

We have developed an effective tool for predicting the risk of cerebral infarction. This tool can help clinicians identify high-risk patients early, and diagnose and treat patients early through personalized risk prediction and intervention. In addition, early intervention, such as controlling risk factors, improving diet and living habits, will benefit patients at high risk of disease at the beginning of treatment[48].

Our current research also has some limitations. First, we only used qRT-PCR to verify the expression level of miRNA, and the study of its mechanism requires more experiments in future research. Second, although the robustness of our nomogram has been extensively checked by internal verification using guided procedure testing, external verification cannot be performed. Third, the generality of other cerebral infarction populations in other regions and countries is uncertain. It requires external evaluation in the wider population of cerebral infarction.

Conclusions

The current results indicated that hematopoietic cell lineage, cell adhesion molecules, phagosomes, and T cell receptor signaling pathways were important pathways in IS. MiR-140-3p, miR-34c-5p, and miR-330-3p may play a pivotal role in the pathogenesis and progression of IS, and may be potential new therapeutic targets for IS.

Abbreviations

miRNA
microRNA
DEmiRNA
Differentially expressed miRNA
DEmRNAs
differentially expressed mRNAs
TFs
transcription factors
GO
Gene Ontology
KEGG
Kyoto Encyclopedia of Genes and Genomes
ceRNA
competitive endogenous RNA
SVM
support vector machine
IS
ischemic stroke
MRI
magnetic resonance imaging
CT
computed tomography
qRT-PCR
quantitative reverse transcription polymerase chain reaction

GEO
Gene Expression Omnibus
BP
biological processes
CC
cell composition
MF
molecular functions
ROC
receiver operating characteristic.

Declarations

We declare that all experimental protocols have been approved by the Ethics Committee of the Fourth Hospital of Hebei Medical University.

We declare that all experimental methods were performed in accordance with guidelines and regulations.

We confirmed that the experiment had obtained informed consent from all participants and that all participants were over 16 years old.

Acknowledgements

None.

Author contributions

G.M. and G.L. conceived and designed the analysis; G.M. wrote the manuscript; W.Y. and L.C. provided the study materials or patients; M.L. and Z.X. performed the collection and assembly of data; C.L. and Z.Q. contributed to the interpretation of the results. All authors discussed the results and approved to the final manuscript.

Competing interests

The authors declare no competing interests.

Availability of Data and Materials

The datasets analysed during the current study are available in the GEO repository, [GSE55937 and GSE16561].

References

1. Lo, E. H., Dalkara, T. & Moskowitz, M. A. Mechanisms, challenges and opportunities in stroke. Nat Rev Neurosci **4**, 399–415, doi:10.1038/nrn1106 (2003).
2. Mortality, G. B. D. & Causes of Death, C. Global, regional, and national life expectancy, all-cause mortality, and cause-specific mortality for 249 causes of death, 1980–2015: a systematic analysis for the Global Burden of Disease Study 2015. Lancet **388**, 1459–1544, doi:10.1016/S0140-6736(16)31012-1 (2016).
3. Latchaw, R. E. *et al.* Recommendations for imaging of acute ischemic stroke: a scientific statement from the American Heart Association. Stroke **40**, 3646–3678, doi:10.1161/STROKEAHA.108.192616 (2009).
4. Ameres, S. L. & Zamore, P. D. J. N. r. M. c. b. Diversifying microRNA sequence and function. **14**, 475–488 (2013).
5. Shao, N.-Y. *et al.* Comprehensive survey of human brain microRNA by deep sequencing. BMC genomics **11**, 1–14 (2010).
6. Dewdney, B. *et al.* Circulating microRNAs as biomarkers for acute ischemic stroke: a systematic review. Journal of Stroke and Cerebrovascular Diseases **27**, 522–530 (2018).
7. Jeyaseelan, K., Lim, K. Y. & Armugam, A. J. S. MicroRNA expression in the blood and brain of rats subjected to transient focal ischemia by middle cerebral artery occlusion. **39**, 959–966 (2008).
8. Long, G. *et al.* Circulating miR-30a, miR-126 and let-7b as biomarker for ischemic stroke in humans. BMC neurology **13**, 1–10 (2013).
9. Barrett, T. *et al.* NCBI GEO: archive for functional genomics data sets—update. Nucleic acids research **41**, D991-D995 (2012).
10. Pathan, M. *et al.* A novel community driven software for functional enrichment analysis of extracellular vesicles data. Journal of extracellular vesicles **6**, 1321455 (2017).
11. Ashburner, M. *et al.* Gene ontology: tool for the unification of biology. Nature genetics **25**, 25–29 (2000).
12. Kanehisa, M. *et al.* KEGG for linking genomes to life and the environment. Nucleic acids research **36**, D480-D484 (2007).
13. Kanehisa, M. & Goto, S. J. N. a. r. KEGG: kyoto encyclopedia of genes and genomes. Nucleic acids research **28**, 27–30 (2000).
14. Li, J.-H., Liu, S., Zhou, H., Qu, L.-H. & Yang, J.-H. J. N. a. r. starBase v2. 0: decoding miRNA-ceRNA, miRNA-ncRNA and protein–RNA interaction networks from large-scale CLIP-Seq data. Nucleic acids research **42**, D92-D97 (2014).
15. Noble, W. S. J. N. b. What is a support vector machine? Nature biotechnology **24**, 1565–1567 (2006).
16. Sauerbrei, W., Royston, P. & Binder, H. J. S. i. m. Selection of important variables and determination of functional form for continuous predictors in multivariable model building. **26**, 5512–5528 (2007).
17. Friedman, J., Hastie, T. & Tibshirani, R. J. J. o. s. s. Regularization paths for generalized linear models via coordinate descent. Journal of statistical software **33**, 1 (2010).

18. Kidd, A. C. *et al.* Survival prediction in mesothelioma using a scalable Lasso regression model: instructions for use and initial performance using clinical predictors. BMJ Open Respiratory Research **5**, e000240 (2018).
19. Balachandran, V. P., Gonen, M., Smith, J. J. & DeMatteo, R. P. J. T. l. o. Nomograms in oncology: more than meets the eye. **16**, e173-e180 (2015).
20. Iasonos, A., Schrag, D., Raj, G. V. & Panageas, K. S. J. J. o. c. o. How to build and interpret a nomogram for cancer prognosis. Journal of clinical oncology **26**, 1364–1370 (2008).
21. Pencina, M. J. & D'Agostino, R. B. J. S. i. m. Overall C as a measure of discrimination in survival analysis: model specific population value and confidence interval estimation. Statistics in medicine **23**, 2109–2123 (2004).
22. Mizuma, A., You, J. S. & Yenari, M. A. J. S. Targeting reperfusion injury in the age of mechanical thrombectomy. **49**, 1796–1802 (2018).
23. Flemming, A. J. N. R. I. Calming inflammation to prevent stroke damage. **19**, 473–473 (2019).
24. Courties, G. *et al.* Ischemic stroke activates hematopoietic bone marrow stem cells. Circulation research **116**, 407–417 (2015).
25. Yilmaz, G. & Granger, D. N. J. N. r. Cell adhesion molecules and ischemic stroke. **30**, 783–793 (2008).
26. Wolach, B., Gavrieli, R., Roos, D. & Berger-Achituv, S. J. J. o. c. i. Lessons learned from phagocytic function studies in a large cohort of patients with recurrent infections. Journal of clinical immunology **32**, 454–466 (2012).
27. Wolach, B., Sazbon, L., Gavrieli, R., Broda, A. & Schlesinger, M. J. J. o. n. Early immunological defects in comatose patients after acute brain injury. **94**, 706–711 (2001).
28. Ruhnau, J. *et al.* Stroke alters respiratory burst in neutrophils and monocytes. **45**, 794–800 (2014).
29. Gill, D. & Veltkamp, R. J. C. o. i. p. Dynamics of T cell responses after stroke. **26**, 26–32 (2016).
30. Offner, H. & Hurn, P. D. J. T. s. r. A novel hypothesis: regulatory B lymphocytes shape outcome from experimental stroke. Translational stroke research **3**, 324–330 (2012).
31. Wei, D.-z. *et al.* Ellagic acid promotes ventricular remodeling after acute myocardial infarction by up-regulating miR-140-3p. Biomedicine **95**, 983–989 (2017).
32. Jude, J. A. *et al.* miR-140-3p regulation of TNF-α-induced CD38 expression in human airway smooth muscle cells. **303**, L460-L468 (2012).
33. Wei, D.-z. *et al.* Ellagic acid promotes ventricular remodeling after acute myocardial infarction by up-regulating miR-140-3p. **95**, 983–989 (2017).
34. Wang, D. *et al.* Hyperglycemia inhibition of endothelial miR-140-3p mediates angiogenic dysfunction in diabetes mellitus. Journal of Diabetes **33**, 374–382 (2019).
35. Grigelioniene, G. *et al.* Gain-of-function mutation of microRNA-140 in human skeletal dysplasia. Nature medicine **25**, 583–590 (2019).
36. Smieszek, A. *et al.* Metformin increases proliferative activity and viability of multipotent stromal stem cells isolated from adipose tissue derived from horses with equine metabolic syndrome. Cells **8**, 80

(2019).
37. Zhang, J. *et al.* Down-regulation of miR-140-3p can alleviate neonatal repetitive pain in rats via inhibiting TGF-β3. **515**, 627–635 (2019).
38. Zhu, Z.-R. *et al.* MiR-140-3p is involved in in-stent restenosis by targeting C-Myb and BCL-2 in peripheral artery disease. Journal of atherosclerosis and thrombosis, 44024 (2018).
39. Zhao, L. *et al.* MicroRNA-140-5p aggravates doxorubicin-induced cardiotoxicity by promoting myocardial oxidative stress via targeting Nrf2 and Sirt2. Redox biology **15**, 284–296 (2018).
40. Liu, Q. *et al.* Identification of apoptosis-related microRNAs and their target genes in myocardial infarction post-transplantation with skeletal myoblasts. **13**, 1–11 (2015).
41. Xu, X. *et al.* Hypoxia induces downregulation of soluble guanylyl cyclase β1 by miR-34c-5p. Journal of cell science **125**, 6117–6126 (2012).
42. Tu, Y. & Hu, Y. J. M. B. D. MiRNA-34c-5p protects against cerebral ischemia/reperfusion injury: involvement of anti-apoptotic and anti-inflammatory activities. Metabolic Brain Disease, 1–11 (2021).
43. Yuan, L., Xu, H., Guo, R., Lu, T. & Li, X. J. B. Long non-coding RNA ZFAS1 alleviates bupivacaine-induced neurotoxicity by regulating the miR-421/zinc finger protein564 (ZNF564) axis. Bioengineered **12**, 5231–5240 (2021).
44. Peng, C., Zhang, C., Su, Z. & Lin, D. J. J. o. c. p. DGCR5 attenuates neuropathic pain through sponging miR-330-3p and regulating PDCD4 in CCI rat models. Journal of cellular physiology **234**, 7292–7300 (2019).
45. Wei, L. *et al.* Beliefs about medicines and non-adherence in patients with stroke, diabetes mellitus and rheumatoid arthritis: a cross-sectional study in China. BMJ open **7**, e017293 (2017).
46. Boehme, A. K., Esenwa, C. & Elkind, M. S. J. C. r. Stroke risk factors, genetics, and prevention. Circulation research **120**, 472–495 (2017).
47. Imamura, T. *et al.* LDL cholesterol and the development of stroke subtypes and coronary heart disease in a general Japanese population: the Hisayama study. Stroke **40**, 382–388 (2009).
48. Opoku, S. *et al.* Prevalence and risk factors for dyslipidemia among adults in rural and urban China: findings from the China National Stroke Screening and prevention project (CNSSPP). BMC Public Health **19**, 1–15 (2019).

Tables

Table.1. Baseline characteristics of IS patients and healthy control subjects

Characteristics	IS group	Control group	χ2	P value
Total subject, n	40	40	-	-
Sex, male/female	23/17	24/16	0.052	0.82
Age (year)	65.900±13.978	61.800±10.939	-	0.148
TG (mmol/L)	1.833±0.537	1.695±0.649	-	0.304
CHO (mmol/L)	5.110±1.141	3.638±1.116	-	<0.001*
HDL-C (mmol/L)	1.233±0.324	1.312±0.303	-	0.261
LDL-C (mmol/L)	2.89±1.00	2.115±0.587	-	<0.001*
Hypertension, n (%)	19□47.5□	8(20)	6.765	0.009*
Diabetes, n (%)	15(37.5)	7(17.5)	4.013	0.045*
Hyperlipidemia, n (%)	6(15)	5(12.5)	0.105	0.745

*P < .05.

Figures

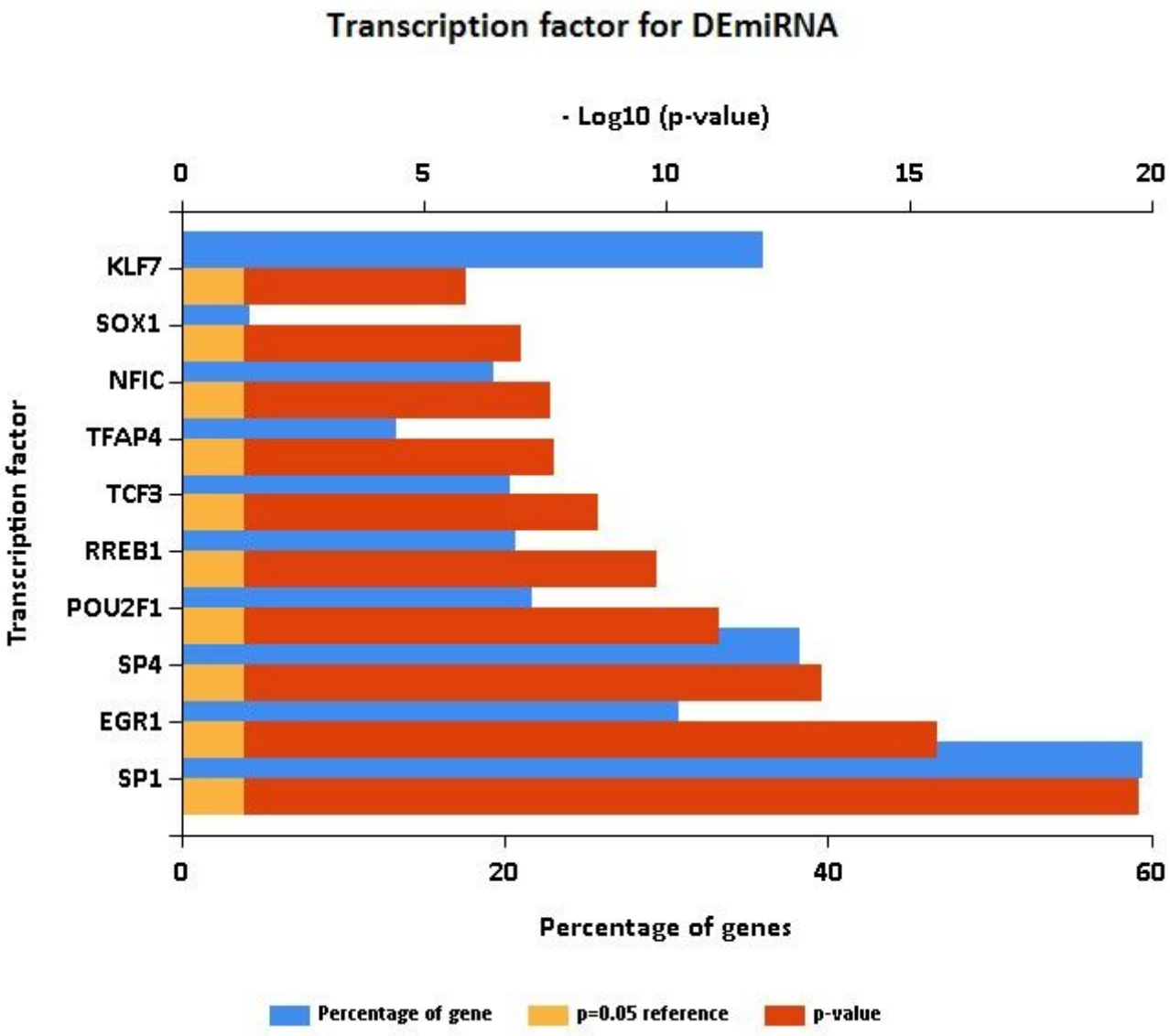

Figure 1

Enrichment analysis of TFs.

Y-axis shows the name of the TFs; The abscissa shows the degree of enrichment of TFs and the percentage of the miRNA, respectively.

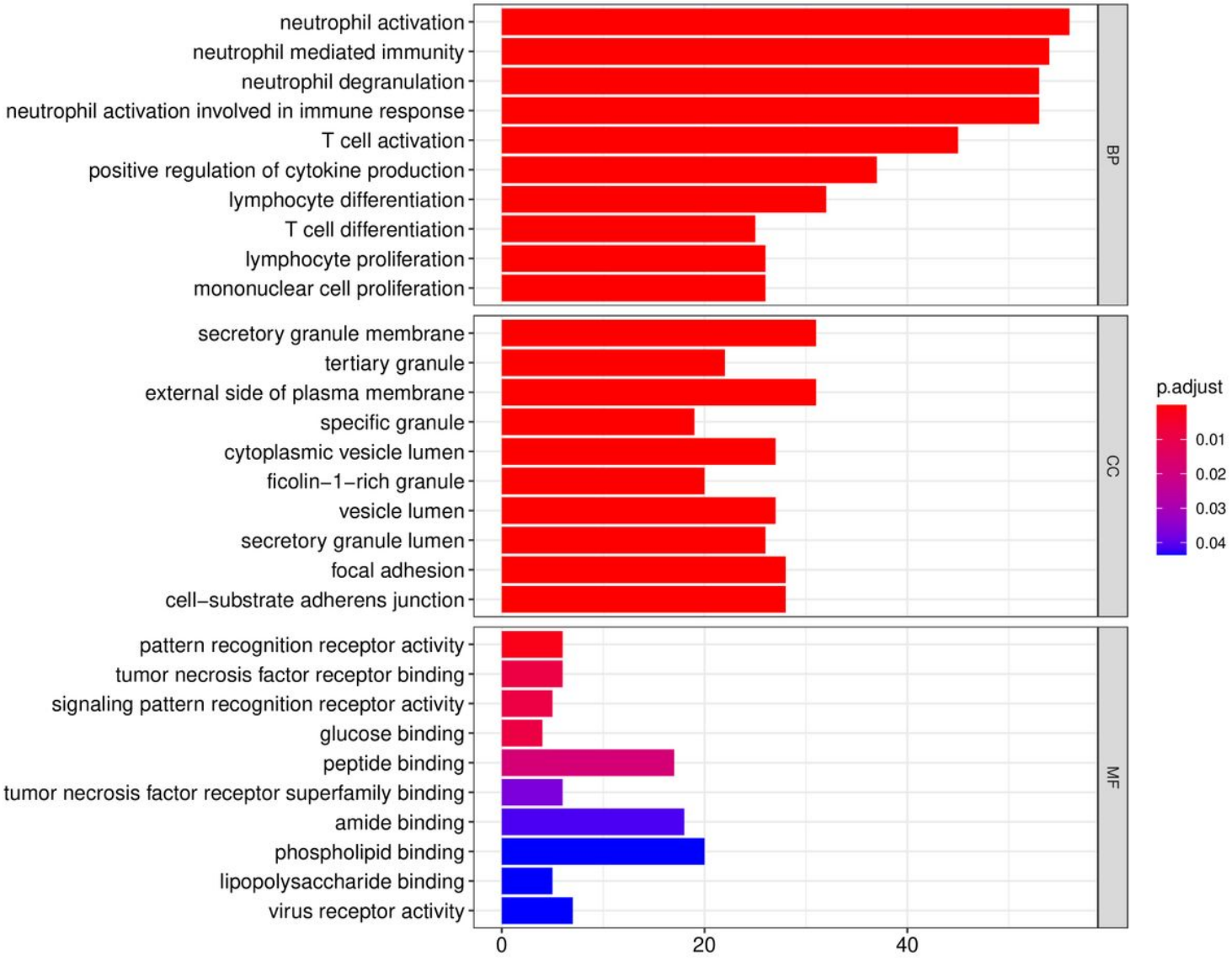

Figure 2

Bar chart for GO enrichment of the DEmRNAs.

The red the color and the longer the shape of the column representing the item, the higher the degree of enrichment.

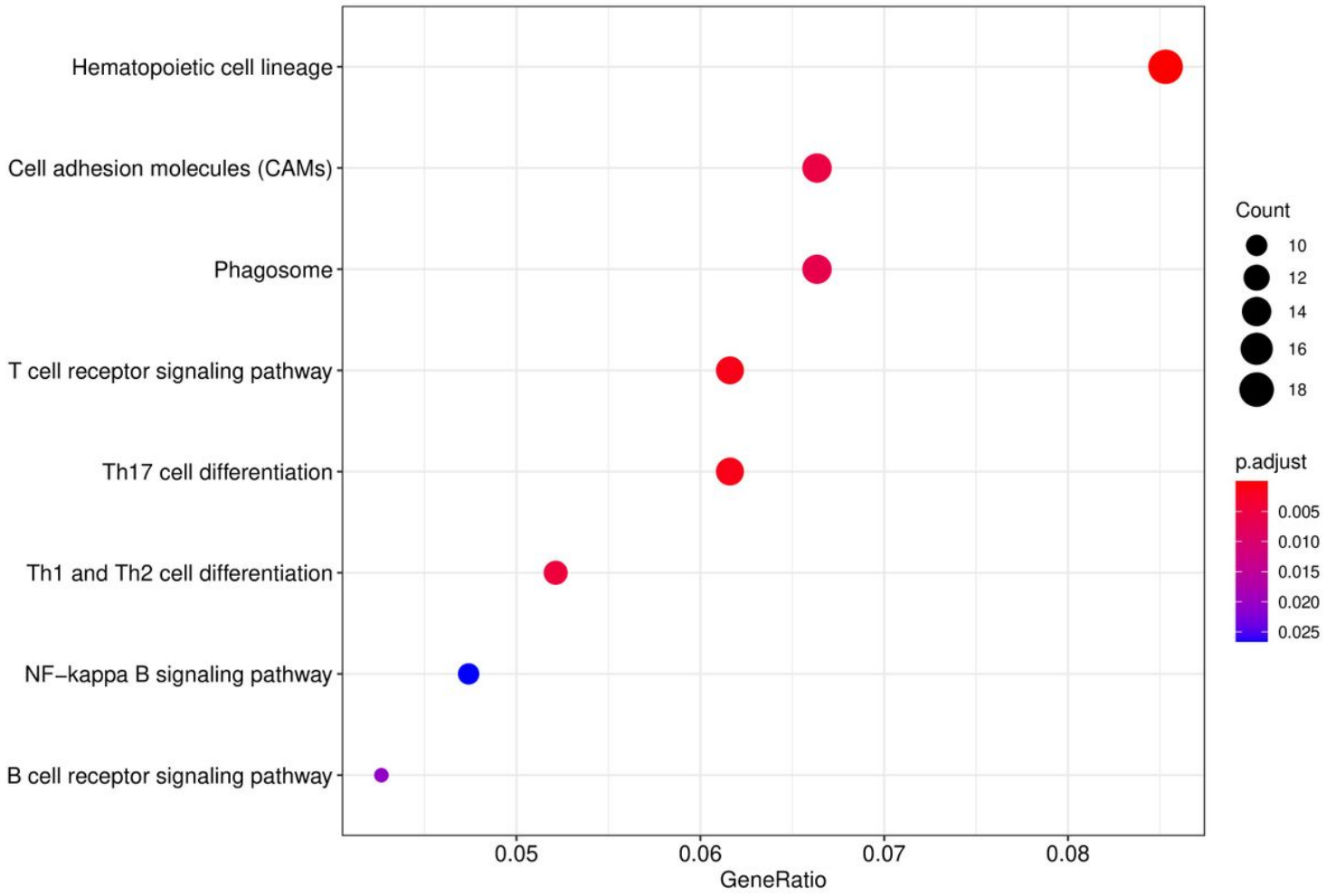

Figure 3

Bubble diagram for KEGG enrichment of the DEmRNAs.

The more red and the larger the shape of the circle representing the item, the higher the degree of enrichment.

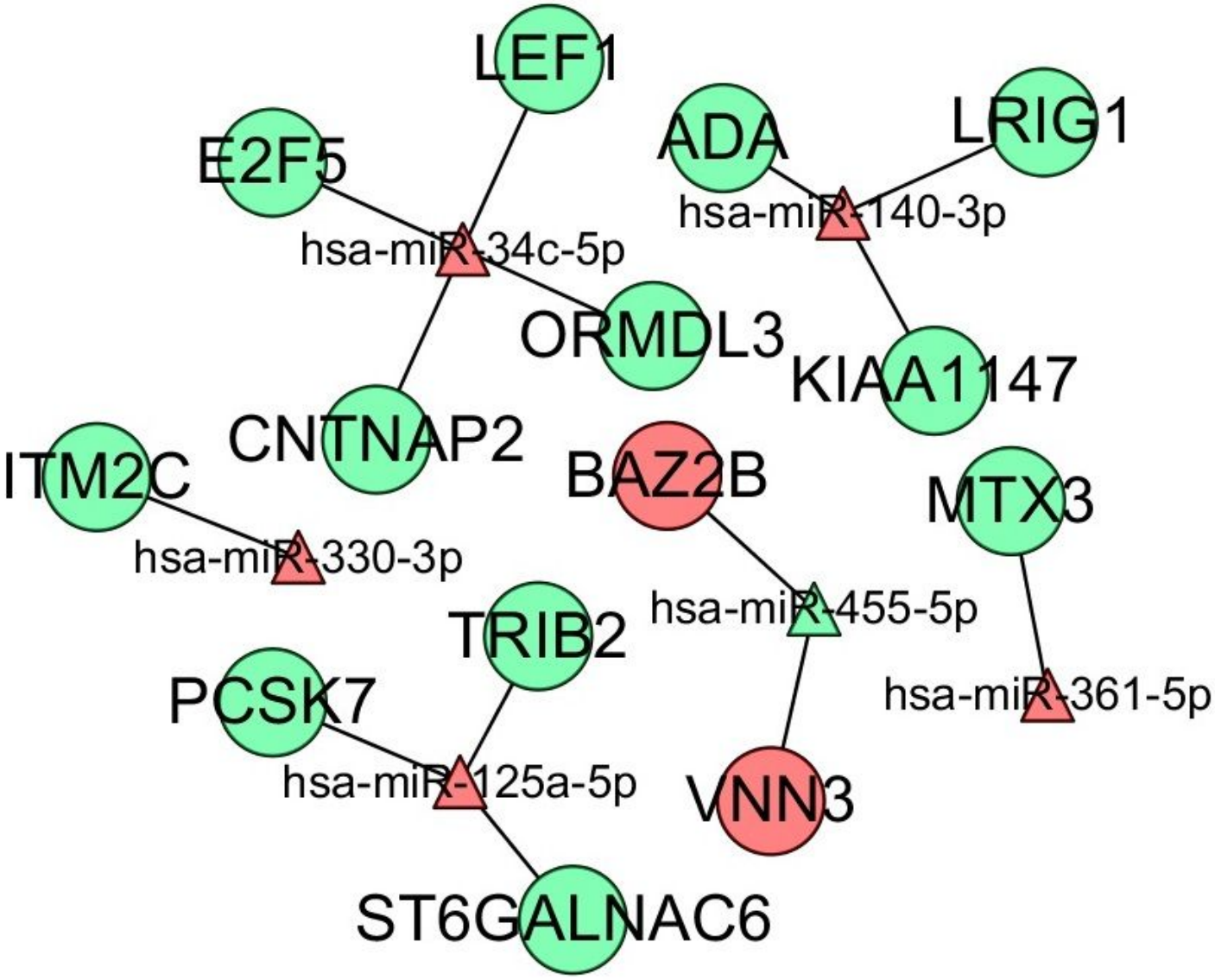

Figure 4

DEmiRNA-DEmRNA interaction network.

Circles represent genes and triangles represent miRNAs. Red shows up-regulated in the experimental group; green shows down-regulated in the experimental group.

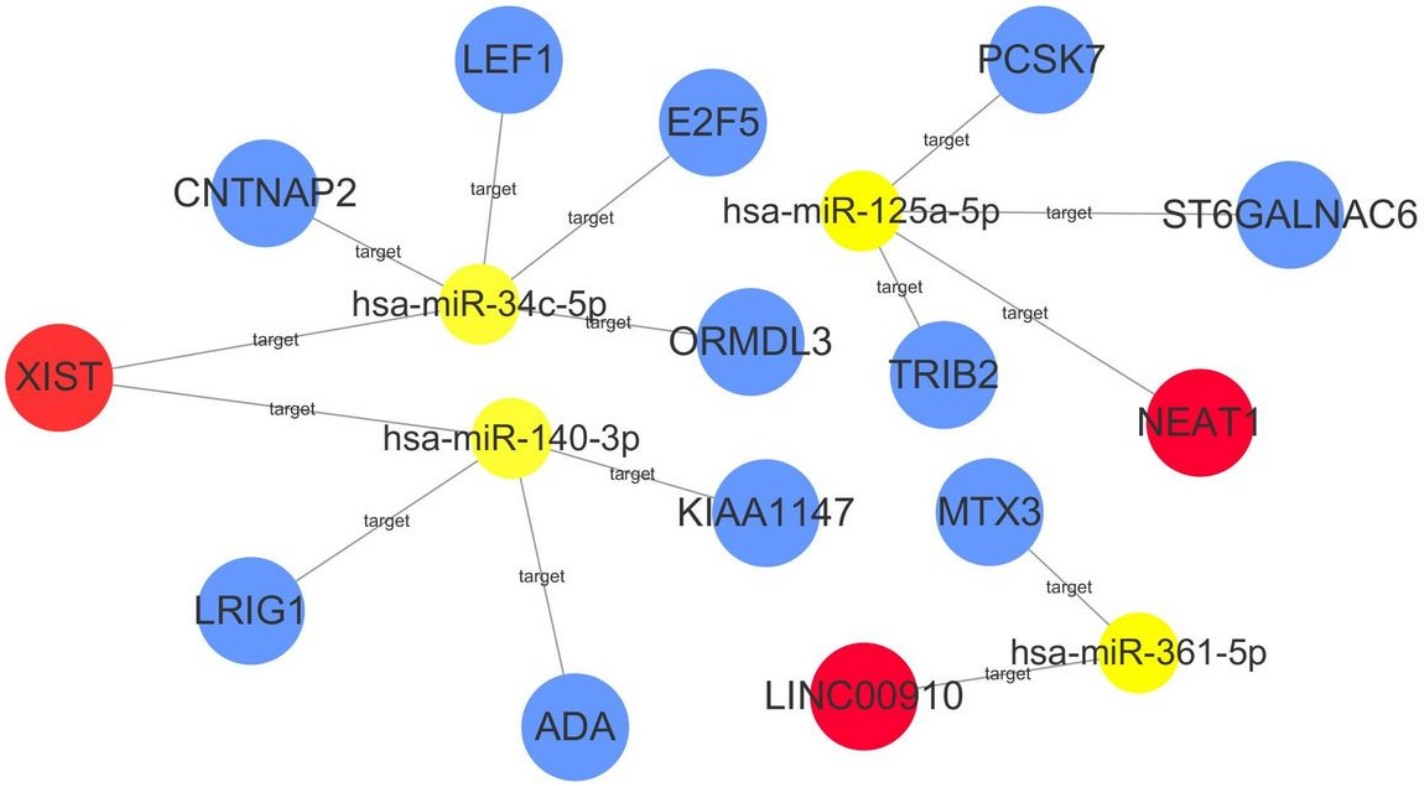

Figure 5

ceRNA network.

Yellow represents miRNAs, blue represents mRNAs, red is LncRNAs.

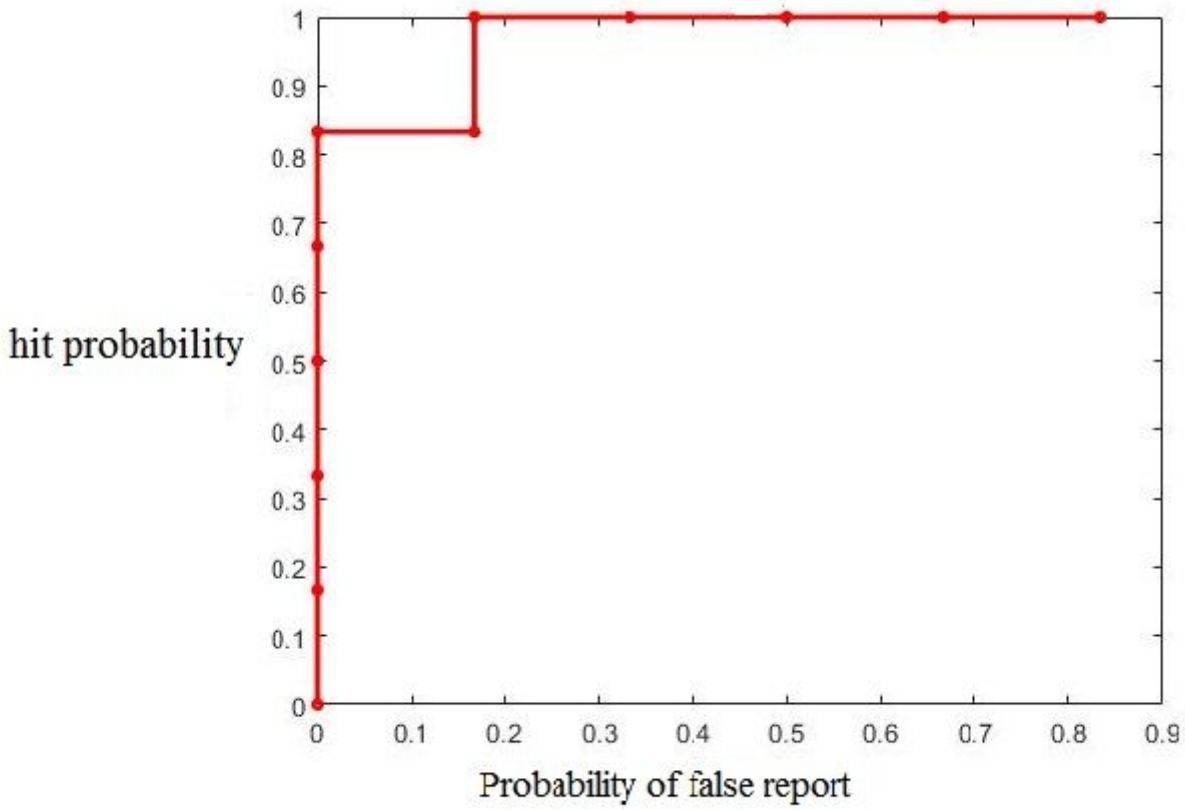

Figure 6

Analysis of ROC of SVM model.

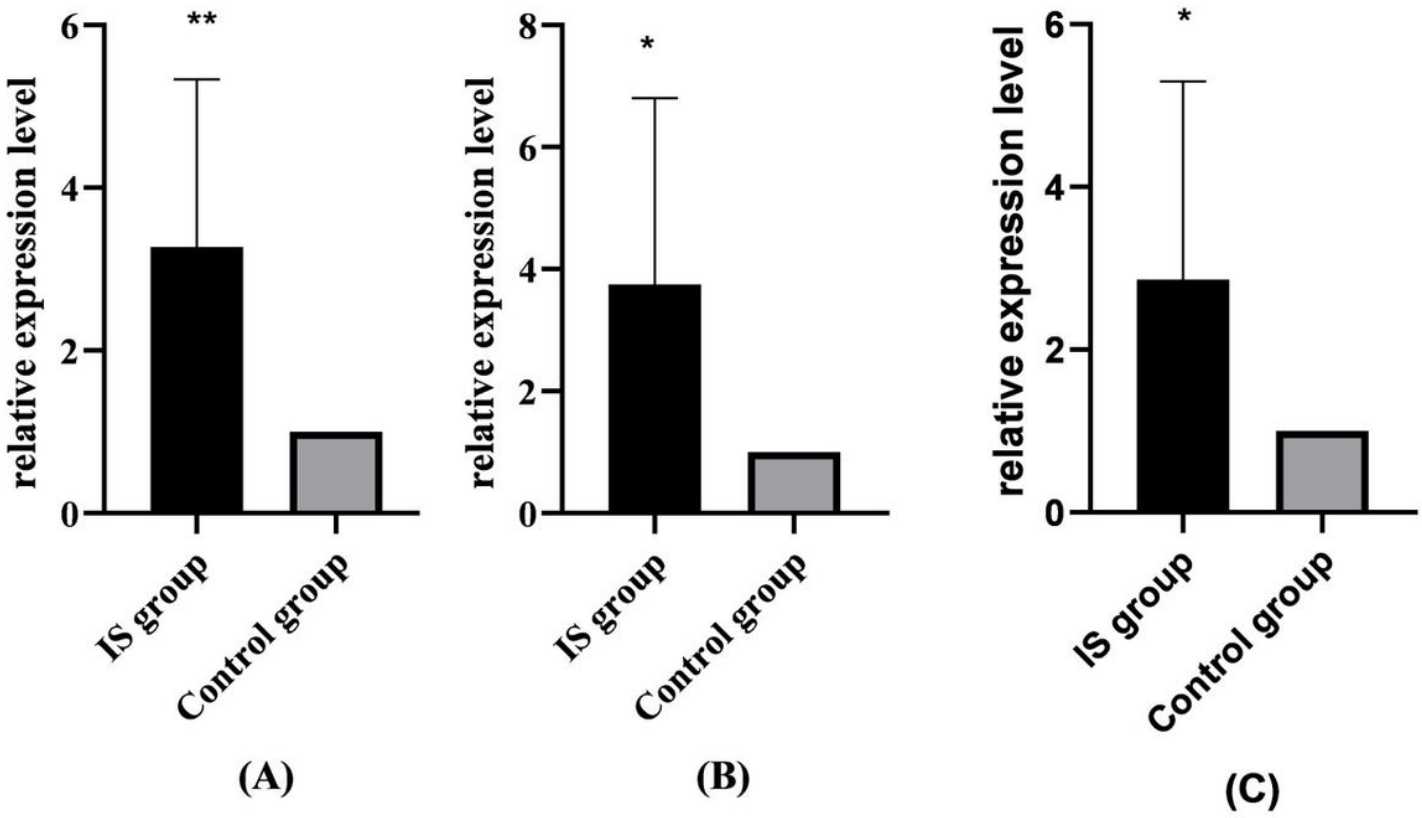

Figure 7

The relative expression level of miR-34c-5p (A), miR-140-3p (B), miR-330-3p (C). * represents $p < 0.05$, and ** represents $p < 0.01$.

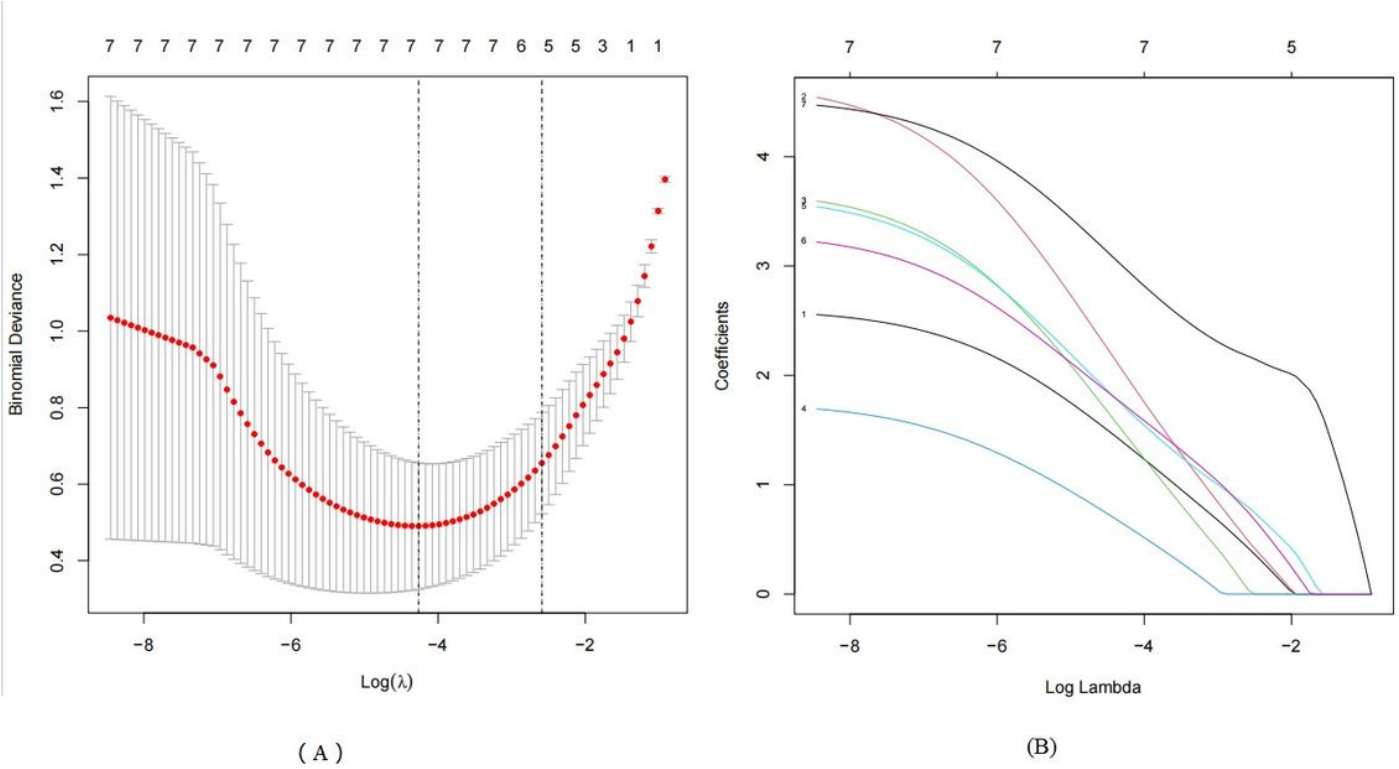

Figure 8

Selection of clinical features using LASSO binary logistic regression model.

(A) Choose the optimal parameter (lambda) in the LASSO model. (B) LASSO coefficient map for 6 features.

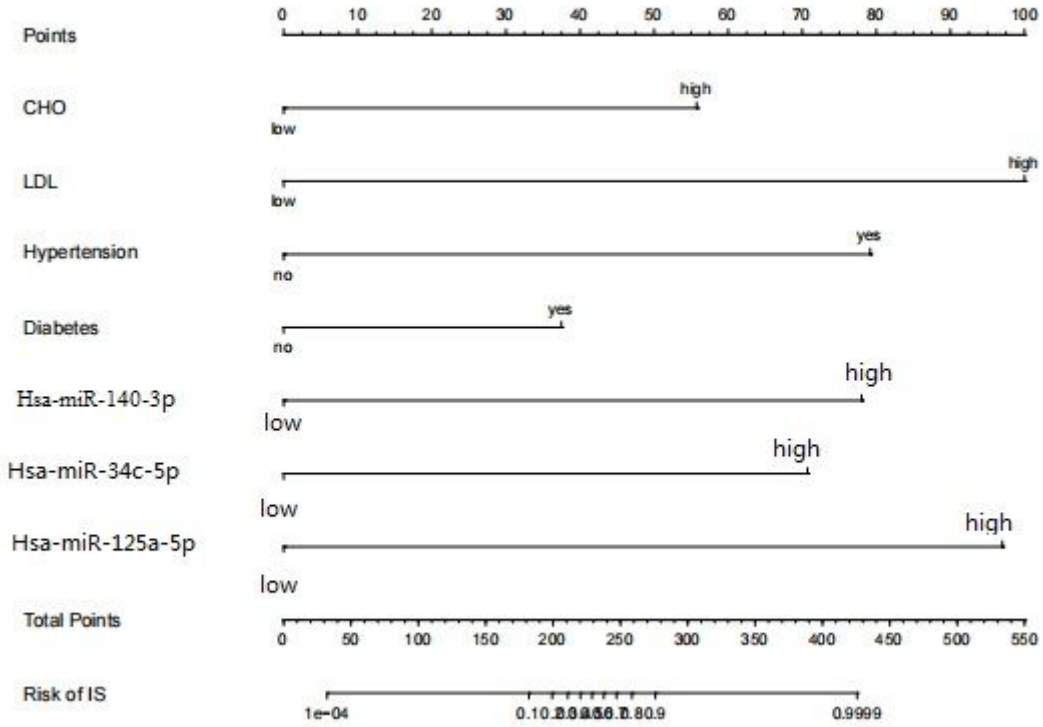

Figure 9

Developed a risk nomogram.

The risk nomogram was developed in the cohort, with the level of cholesterol, level of low-density lipoprotein, high or low blood pressure, miR-34c-5p, miR-140-3p, and miR-330-3p expression.

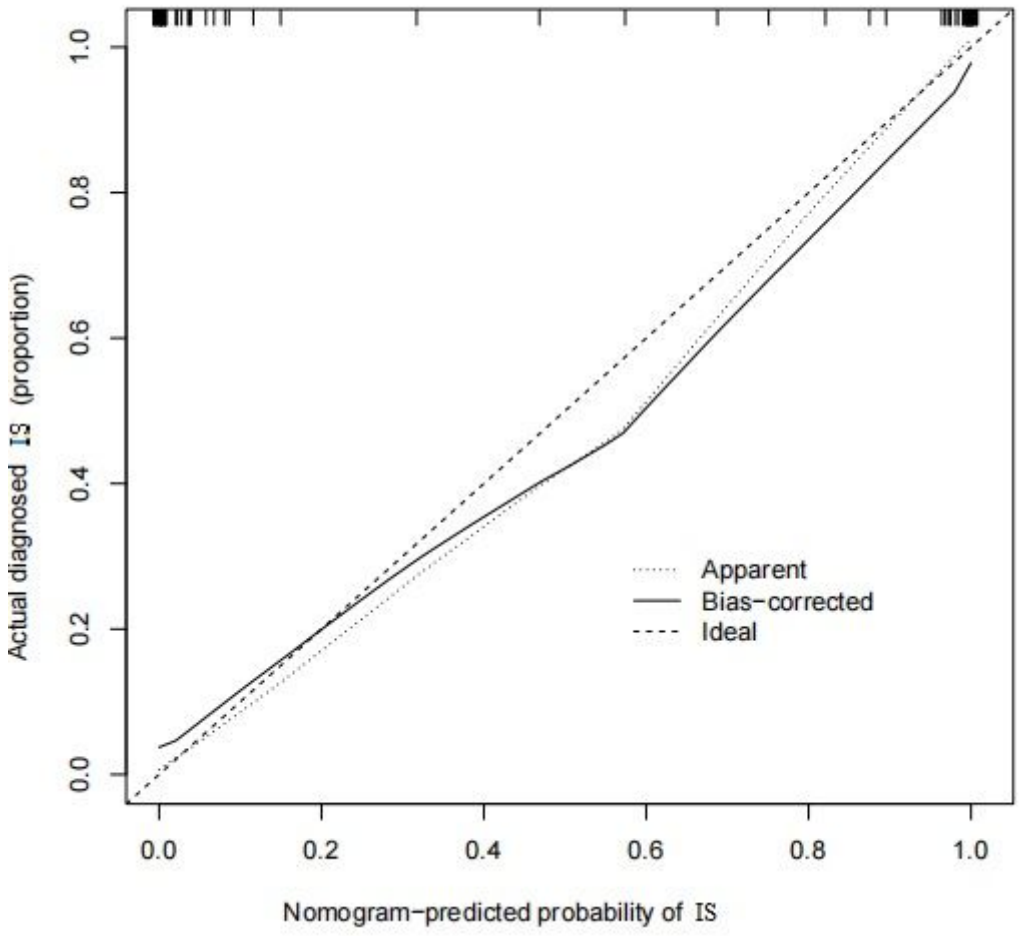

Figure 10

Calibration curve for nomogram to predict IS risk.

The x-axis shows the predicted risk. The y-axis shows the actual diagnosis. The solid line is a performance demonstration of the nomogram, where the dashed line closer to the diagonal indicates better prediction.

Supplementary Files

This is a list of supplementary files associated with this preprint. Click to download.

- Supplementary1.xls
- Supplementary2.xls
- Supplementarytable1.docx